X-ray Multi-Photon Multiple Ionization

Ludger Inhester
Center for Free-Electron Laser Science CFEL,
Deutsches Elektronen-Synchrotron DESY

June 10, 2024

Project Goal

In this project, the participants will learn to model multiphoton multiple ionization dynamics of atoms exposed to intense x-ray radiation. The participants will evaluate crucial quantities and pulse-parameter dependencies that are relevant for high-intensity AMO experiments at XFEL sources. Such theoretical modelling is often applied at experiments where multiple x-ray ionization occurs, for example in Refs. [6, 4, 2, 1].

Preparations

You need to install the XATOM software, which is part of XRAYPAC. Please find instructions to download and install XRAYPAC on the website `https://www.desy.de/~xraypac`. The content of this exercise and all required files may be obtained from `https://gitlab.desy.de/CDT/tutorialratesolving.git`.
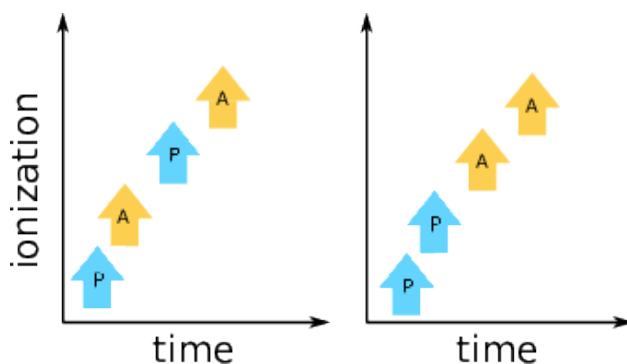
1 Rate Equation

Figure 1: The XFEL pulse ionizes an atom via sequences of core-shell photoionization (P) and Auger decay (A). The left example shows the sequence PAPA, the right example shows the sequence PPAA. Adapted from Ref. [6].

The intense x-ray light in an XFEL pulse can ionize the sample many times. When molecules or atoms are exposed to such pulses, the overall dynamics can be modelled via sequential steps

that describe a series of photoionization, Auger decay, and fluorescence processes. Such sequences (without fluorescence) are sketched in Fig. 1.

The involved multiphoton multiple ionization dynamics can be modeled to a good approximation via rate equations of the type

$$\frac{d}{dt}p_i(t) = \sum_{j}^{j \neq i} \gamma_{j \to i}(t)p_j(t) - \gamma_{i \to j}(t)p_i(t), \tag{1}$$

where $p_i(t)$ is the time-dependent population of an electronic configuration i and $\gamma_{j \to i}(t)$ is a transition rate for a process between configuration j and i. In this exercise, we consider the following types of processes:

- Photoionization: The rate is given $\gamma_{j \to i}(t) = \sigma_{j \to i}J(t)$, i.e., the product of the corresponding photoionization cross section and photon flux $J(t)$.

- Auger-Meitner decay: The rate is given by the corresponding Auger-Meitner decay rate $\gamma_{j \to i}(t) = \Gamma_{j \to i}$.

- Fluorescence: The rate is given by the corresponding fluorescence decay rate $\gamma_{j \to i}(t) = \Gamma_{j \to i}$.

Exercise 1

Motivation: Analytically solve the rate equation, derive dependecies for the competition of photoionization and Auger-Meitner decay.
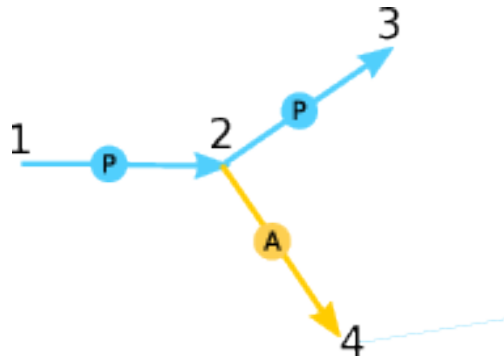

Figure 2: Illustration of the competing pathways: Photoionization vs. Auger-Meitner decay step following photoionzation.

Given is the following set of rate equations:

$$\begin{aligned}
\frac{d}{dt}p_1(t) &= -\sigma\,J(t)\,p_1(t), \\
\frac{d}{dt}p_2(t) &= \sigma\,J(t)\,p_1(t) - \sigma\,J(t)\,p_2(t) - \Gamma p_2(t) \\
\frac{d}{dt}p_3(t) &= \sigma\,J(t)\,p_2(t), \\
\frac{d}{dt}p_4(t) &= \Gamma\,p_2(t),
\end{aligned}$$

with the boundary conditions $p_1(0) = 1$, $p_2(0) = 0$, $p_3(0) = 0$, $p_4(0) = 0$, and a temporal step-function for the fluence,

$$J(t) = \begin{cases} 0 & \text{if } t \leq 0 \\ J & \text{if } t > 0 \end{cases}.$$

This set of rate equations models the competition between Auger-Meitner decay and photoionization illustrated in Fig. 2: The ionization dynamics start with photoionization from electronic configuration 1 into configuration 2. Configuration 2 can either further be photoionized into configuration 4 (a PP sequence) or undergo Auger-Meitner decay into configuration 3 (a PA sequence). The possible pathways are also illustrated by the graph on the right hand side of the rate equation.

Give the analytical solution and plot them for varying parameters σJ and Γ. Help: For $p_2(t)$, you may consider the ansatz $p_2(t) = \lambda(t) \exp(-(\sigma J + \Gamma)t)$. Alternatively, you may consider using the Laplace transformation. What is the probability to observe PP vs. PA process?

Solution

$p_1(t)$ can be solved by separation of variables and integration. The solution is ($t \geq 0$)

$$p_1(t) = \exp(-\sigma J t).$$

This yields for $p_2(t)$, $t \geq 0$

$$\frac{d}{dt}p_2(t) = -(\sigma J + \Gamma)\, p_2(t) + \sigma J \exp(-\sigma J t),$$

which is an inhomogeneous first-order differential equation. It can be solved employing the Ansatz $p_2(t) = \lambda(t) \exp(-\beta t)$, with $\beta = \sigma J + \Gamma$ (homogeneous solution + variation of constant). This yields

$$e^{-\beta t}\frac{d}{dt}\lambda(t) - \beta e^{-\beta t}\lambda(t) = -\beta \lambda(t)e^{-\beta t} + \sigma J\, e^{-\sigma J t},$$

$$\frac{d}{dt}\lambda(t) = \sigma J\, e^{(\beta - \sigma J)t} \Rightarrow \lambda(t) = \frac{\sigma J}{\beta - \sigma J}\, e^{(\beta - \sigma J)t} + c$$

$$\Rightarrow p_2(t) = \left[\frac{\sigma J}{\beta - \sigma J}\, e^{(\beta - \sigma J)t} + c\right] e^{-\beta t}.$$

Inserting the boundary condition yields

$$p_2(0) = \frac{\sigma J}{\beta - \sigma J} + c = 0 \Rightarrow c = -\frac{\sigma J}{\beta - \sigma J}$$

$$\Rightarrow p_2(t) = \frac{\sigma J}{\Gamma}\left(e^{-\sigma J t} - e^{-(\sigma J + \Gamma)t}\right).$$

The solution for $p_3(t)$ is obtained as follows:

$$\frac{d}{dt}p_3(t) = \frac{\sigma^2 J^2}{\Gamma}\left(e^{-\sigma J t} - e^{-(\sigma J + \Gamma)t}\right),$$

$$p_3(t) = \frac{\sigma^2 J^2}{\Gamma}\left(-\frac{1}{\sigma J}e^{-\sigma J t} + \frac{1}{\sigma J + \Gamma}e^{-(\sigma J + \Gamma)t}\right) + c.$$

Inserting the boundary condition,

$$p_3(0) = 0, \tag{2}$$

yields

$$p_3(0) = \frac{\sigma^2 J^2}{\Gamma}\left(-\frac{1}{\sigma J} + \frac{1}{\sigma J + \Gamma}\right) + c = 0 \Rightarrow c = \frac{\sigma J}{\sigma J + \Gamma}$$

$$\Rightarrow p_3(t) = \frac{\sigma J}{\sigma J + \Gamma} - \frac{\sigma J}{\Gamma}e^{-\sigma J t} + \frac{\sigma^2 J^2}{\sigma J \Gamma + \Gamma^2}e^{-(\sigma J + \Gamma)t}.$$

The solution for $p_4(t)$ with $t \geq 0$ is obtained as follows:

$$\frac{d}{dt}p_1(t) + p_2(t) + p_3(t) + p_4(t) = 0, \text{ and } p_1(0) + p_2(0) + p_3(0) + p_4(0) = 1$$

$$\Rightarrow p_1(t) + p_2(t) + p_3(t) + p_4(t) = 1$$

$$\Rightarrow p_4(t) = 1 - p_1(t) - p_2(t) - p_3(t)$$

$$\Rightarrow p_4(t) = 1 - e^{-\sigma J t} - \frac{\sigma J}{\Gamma}e^{-\sigma J t} + \frac{\sigma J}{\Gamma}e^{-(\sigma J + \Gamma)t} - \frac{\sigma J}{\sigma J + \Gamma} + \frac{\sigma J}{\Gamma}e^{-\sigma J t} - \frac{\sigma^2 J^2}{\sigma J \Gamma + \Gamma^2}e^{-(\sigma J + \Gamma)t}$$

$$= 1 - e^{-\sigma J t} - \frac{\sigma J}{\sigma J + \Gamma}\left(1 - e^{-(\sigma J + \Gamma)t}\right).$$
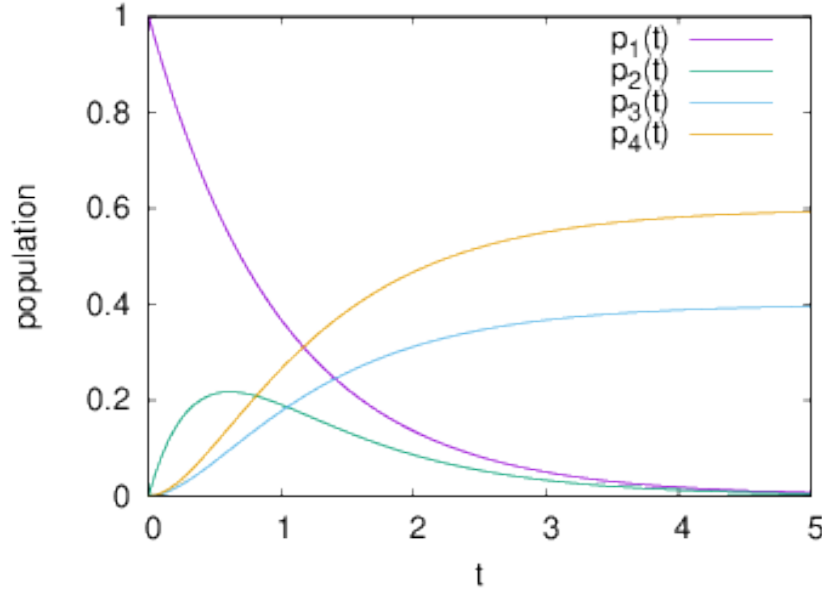

Figure 3: Example for $p_1(t)$, $p_2(t)$, $p_3(t)$, and $p_4(t)$ for $\sigma J = 1$ and $\Gamma = 3/2$

Alternatively, the solution can be obtained via Laplace transformation. Consider the Laplace transformation

$$\tilde{f}(s) = \mathcal{L}(f(t)) = \int_0^\infty f(t)e^{-st}dt \tag{3}$$

and the back-transformation

$$f(t) = \mathcal{L}^{(-1)}(\tilde{f}(s)) = \frac{1}{2\pi i}\int_{\gamma - i\infty}^{\gamma + i\infty} \tilde{f}(s)e^{st}ds, \tag{4}$$

where the parameter γ is larger than the real part of any singularity of $\tilde{f}(s)$. It holds that

$$\mathcal{L}\left(\frac{d}{dt}f(t)\right) = s\tilde{f}(s) - f(0). \tag{5}$$

Using the Laplace transformation, the coupled rate equations for $t \geq 0$ can be written as

$$
\begin{aligned}
s\tilde{p}_1(s) &= 1 - \sigma J \tilde{p}_1(s), \\
s\tilde{p}_2(s) &= \sigma J \tilde{p}_1(s) - \sigma J \tilde{p}_2(s) - \Gamma\tilde{p}_2(s) \\
s\tilde{p}_3(s) &= \sigma J \tilde{p}_2(s), \\
s\tilde{p}_4(s) &= \Gamma \tilde{p}_2(s),
\end{aligned}
$$

This can be directly solved and back-transformed:

$$\tilde{p}_1(s) = \frac{1}{s + \sigma J}$$

$$\Rightarrow p_1(t) = \exp(-\sigma Jt)$$

$$\tilde{p}_2(s) = \frac{\sigma J}{(s + \Gamma + \sigma J)} \tilde{p}_1(s) = \frac{\sigma J}{(s + \Gamma + \sigma J)} \frac{1}{(s + \sigma J)} = \frac{\sigma J}{\Gamma}\left(-\frac{1}{s + \Gamma + \sigma J} + \frac{1}{s + \sigma J}\right)$$

$$\Rightarrow p_2(t) = \frac{\sigma J}{\Gamma}\left(\exp(-\sigma Jt) - \exp(-(\sigma J - \Gamma)t)\right)$$

$$\tilde{p}_3(s) = \frac{\sigma J}{s}\tilde{p}_2(s) = \frac{(\sigma J)^2}{\Gamma}\frac{1}{s}\left(-\frac{1}{s + \Gamma + \sigma J} + \frac{1}{s + \sigma J}\right)$$

$$= \frac{(\sigma J)^2}{\Gamma}\left(\left(-\frac{1}{\Gamma + \sigma J} + \frac{1}{\sigma J}\right)\frac{1}{s} + \frac{1}{(\Gamma + \sigma J)}\frac{1}{(s + \Gamma + \sigma J)} - \frac{1}{\sigma J}\frac{1}{(s + \sigma J)}\right)$$

$$\Rightarrow p_3(t) = \frac{(\sigma J)^2}{\Gamma}\left(\left(-\frac{1}{\Gamma + \sigma J} + \frac{1}{\sigma J}\right) + \frac{1}{\Gamma + \sigma J}\exp\left(-(\Gamma + \sigma J)t\right) - \frac{1}{\sigma J}\exp\left(-\sigma Jt\right)\right)$$

$$\tilde{p}_4(s) = \frac{\Gamma}{s}\tilde{p}_2(s) = \frac{\sigma J}{s}\left(-\frac{1}{s + \Gamma + \sigma J} + \frac{1}{s + \sigma J}\right)$$

$$= \sigma J\left(\left(-\frac{1}{\Gamma + \sigma J} + \frac{1}{\sigma J}\right)\frac{1}{s} + \frac{1}{(\Gamma + \sigma J)}\frac{1}{(s + \Gamma + \sigma J)} - \frac{1}{\sigma J}\frac{1}{(s + \sigma J)}\right)$$

$$\Rightarrow p_4(t) = \sigma J\left(\left(-\frac{1}{\Gamma + \sigma J} + \frac{1}{\sigma J}\right) + \frac{1}{\Gamma + \sigma J}\exp\left(-(\Gamma + \sigma J)t\right) - \frac{1}{\sigma J}\exp\left(-\sigma Jt\right)\right)$$

In this example, the probability to observe PA or PP process is directly given by the populations p_3 and p_4 at $t \to \infty$.

$$p_3(t \to \infty) = \frac{\sigma J}{\sigma J + \Gamma} \quad p_4(t \to \infty) = 1 - \frac{\sigma J}{\sigma J + \Gamma}$$

$$P_{\text{PP}}/P_{\text{PA}} = \frac{p_3(t \to \infty)}{p_4(t \to \infty)} = \frac{\sigma J}{\sigma J + \Gamma}\bigg/\left(1 - \frac{\sigma J}{\sigma J + \Gamma}\right) = \frac{\sigma J}{\Gamma}.$$

2   Calculate Decay Rates and Cross Sections

The transition rates for the electronic processes can be calculated using ab-initio methods. Here a short overview of the basic equations is given. See Ref. [3] for further details.

The photoionization cross section (in dipole approximation and assuming effectively independent electrons) is given by

$$\sigma_{i \to f} = \frac{4\pi^2}{\omega} \alpha \, \delta(E_f - E_i - \omega) \, |\langle \phi_f | \hat{\epsilon} \cdot \nabla | \phi_i \rangle|^2, \tag{6}$$

where ω is the photon energy, E_f and E_i are the effective one-particle energies, ϕ_f and ϕ_i are the corresponding one-electron wavefunctions, $\hat{\epsilon}$ is the polarization vector of the light field, and $\nabla = (\partial_x, \partial_y, \partial_z)^T$.

Employing similar approximations on the electronic wave function, the Auger-Meitner decay rate from an initial electronic state with a core vacancy in orbital $\phi_c(\mathbf{r})$ (otherwise closed shell) and a final electronic state with two vacancies in $\phi_{v_1}(\mathbf{r})$ and $\phi_{v_2}(\mathbf{r})$ and an Auger-Meitner electron with continuum wave function $\phi_k(\mathbf{r})$ is given by

$$\Gamma_{i \to f} = 2\pi\delta(E_{v_1} + E_{v_2} - E_c - E_k) \begin{cases} |\langle v_1 v_1 | \frac{1}{r} | ck \rangle|^2 & \text{if } v_1 = v_2, \\ \frac{1}{2}|\langle v_1 v_2 | \frac{1}{r} | ck \rangle + \langle v_2 v_1 | \frac{1}{r} | ck \rangle|^2 & \text{if } v_1 \neq v_2, \text{singlet spin config. ,} \\ \frac{3}{2}|\langle v_1 v_2 | \frac{1}{r} | ck \rangle - \langle v_2 v_1 | \frac{1}{r} | ck \rangle|^2 & \text{if } v_1 \neq v_2, \text{triplet spin config.} \end{cases} \tag{7}$$

where

$$\langle v_1 v_2 | \frac{1}{r} | ck \rangle = \int dr_1 \int dr_2 \, \phi_{v_1}^*(\mathbf{r}_1) \phi_{v_2}^*(\mathbf{r}_2) \frac{1}{|\mathbf{r}_1 - \mathbf{r}_2|} \phi_c(\mathbf{r}_1) \phi_k(\mathbf{r}_2), \tag{8}$$

and E_{v_1}, E_{v_2}, E_c, and E_k are the corresponding one-particle energies.

The fluorescence rate is given by

$$\Gamma_{i \to f} = \frac{4\alpha\omega^3}{3} |\langle \phi_f | \mathbf{r} | \phi_i \rangle|^2, \tag{9}$$

where $\omega = E_i - E_f$ is the emitted fluorescence photon energy, and $\langle \phi_f | \mathbf{r} | \phi_i \rangle$ is the transition dipole moment between the the initially occupied orbital ϕ_i and the initially vacant orbital ϕ_f.

The calculation of the respective transition rates can be a challenge on its own. They can be obtained by available electronic structure programs. In this course, we employ the atomic electronic structure program XATOM [5]. XATOM calculates transition rates employing the Hartree-Fock-Slates electronic structure model. All the obtained transition rates are average over the spin-angular terms for a given atomic configuration. For example, the cross section for core-shell ionization of a neutral, ground state carbon atom (configuration $1s^2 2s^2 2p^2$) is a weighted average over all the involved atomic terms ^1S, ^3P, ^1D.

Exercise 2

Motivation: Learn how to use the electronic structure tool XATOM to calculate rates and cross-sections.

Exercise 2a

Make yourself familiar with the XATOM tool. You can calculate the electronic structure of a neon atom by typing

```
$ xatom -s Ne
```

To calculate a specific electronic configuration of neon use

```
$ xatom -s Ne -conf 1s1_2s2_2p6
```

To calculate a photoionization cross section for a given photon energy use

```
$ xatom -s Ne -pcs -PE 1000
```

Decay rates (for Auger-Meitner and fluorescence) can be calculated via

```
$ xatom -s Ne -conf 1s1_2s2_2p6 -decay
```

Moreover, you can get a short overview of command-line options with

```
$ xatom --help
```

Further usage is described in the pdf document "xatom_manual.pdf" in the project folder.

Exercise 2b

Calculate the photoionization cross section for neutral neon and ionized neon as a function of photon energy from $400\,\mathrm{eV}$ to $1000\,\mathrm{eV}$. Plot the results (you may use any plot program you like).

Exercise 2c

Calculate the lifetime of core-ionized (configuration $1s^1 2s^2 2p^6$), doubly core-coreionized (configuration $1s^0 2s^2 2p^6$) neon, and core and valence-ionized neon (e.g., configuration $1s^1 2s^2 2p^0$). Compare the numbers. Can you explain why one is considerably larger?
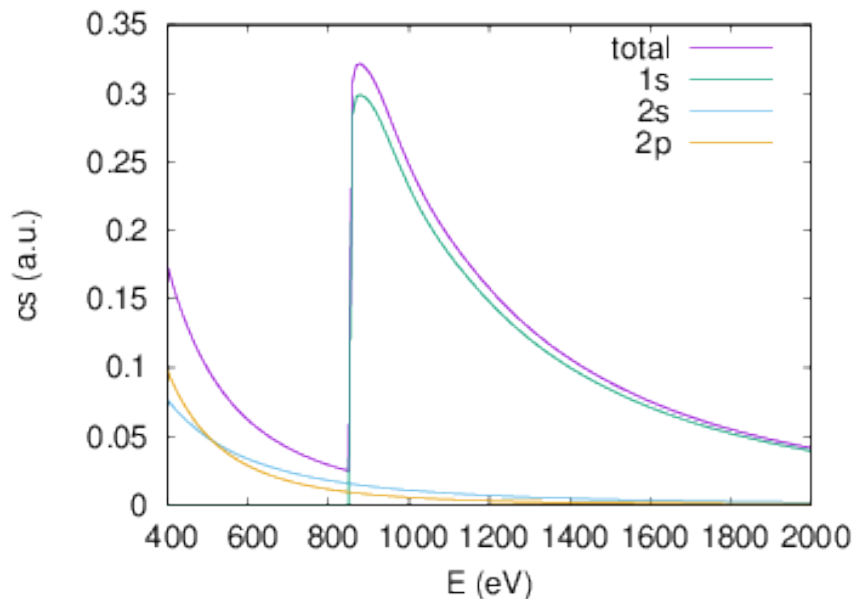

Solution

Figure 4: Calculated total and partial photoionization cross section for neon.

The photoionization cross section shows an edge at $\simeq 860\,\text{eV}$ because at this energy ionization of the $1s$ shell becomes available.

The lifetime of the neon $1s^{-1}$ configuration is $2.5\,\text{fs}$, and the lifetime of the neon $1s^{-2}$ configuration is $0.8\,\text{fs}$, the lifetime of the configuration $1s^1 2s^2 2p^0$ is $13.4\,\text{fs}$. The double-core hole decays much faster because each core hole can be refilled via Auger-Meitner processes. In addition, the double-core-hole lifetime is even shorter than half the single-core-hole lifetime, because of valence orbitals are more tight around the core and thus interaction integrals become larger. Holes in the valence increase the core-hole lifetime because electrons for Auger-Meitner and fluorescence decay channels are missing.

---

3 Solve Rate Equations Numerically

The python notebook `rateSolver_Solution.ipynb`(html) contains a code for numerically solving rate equations. To solve the rate equations with this code, a table of rates and cross sections needs to be prepared that is fed into the numerical solver. The table for the previous 4-configuration example with parameters $\sigma = 1$, $\Gamma = 3/2$, and $J = 1$ is already provided.

For neon, a table of rates and cross sections for a photon energy of $2\,\text{keV}$ is also already provided. It has been generated with the python notebook `tableGeneration.ipynb` (html). Feel free to inspect it. You may also want to modify it to address other elements or further photon energies. In order to use it, you have to set XATOMPATH tp the path of your XATOM binary. Please consider that for larger atoms the number of electronic configurations explodes dramatically. For such atoms, solving the rate equation with tabulated rates thus becomes infeasible and other approaches have to be taken.

Exercise 3

Motivation: Learn how to solve the rate equations for a realistic scenario using numerical solver.

Exercise 3a

Modify the notebook to verify your previous analytical solution with the numerical one. Add the required code into blank cells in the notebook.

Exercise 3b

In the python notebook `rateSolver_Solution.ipynb`(html) the rate equations are solved for the provided table of rates and cross sections for neon. Make yourself familiar with the code. The variable *nPhotonsperSqmuM* specifies the number of photons per μm^2, the variable *fwhmPulse* specifies the full width at half maximum of the temporal pulse profile. Because of the many configurations involved, it is tedious to inspect the solution for every single configuration. Instead, the average charge is shown and the population of charge states (summing up the populations for configurations with the same charge state). The probability for PP vs. PA sequence

is calculated as well. Try to change the parameters fluence and pulse duration and inspect how the results change.

Exercise 3c

Modify the notebook such that you generate plots of the average charge as a function of fluence and as a function of pulse duration. Add your code in the blank cells of the notebook. Plot the average final charge as a function of fluence for a given pulse duration. Plot the average final charge as a function of pulse duration for a given fluence. Plot the ratio of PP processes vs. PA processes as a function of fluence and pulse duration. Explain the observation.

Exercise 3d

Consider the notebook `tableGeneration.ipynb` (html). Can you do your analysis for another photon energy, e.g., $1\,\text{keV}$?

References

[1] T. Jahnke, R. Guillemin, L. Inhester, S.-K. Son, G. Kastirke, M. Ilchen, J. Rist, D. Trabert, N. Melzer, N. Anders, T. Mazza, R. Boll, A. De Fanis, V. Music, Th. Weber, M. Weller, S. Eckart, K. Fehre, S. Grundmann, A. Hartung, M. Hofmann, C. Janke, M. Kircher, G. Nalin, A. Pier, J. Siebert, N. Strenger, I. Vela-Perez, T. M. Baumann, P. Grychtol, J. Montano, Y. Ovcharenko, N. Rennhack, D. E. Rivas, R. Wagner, P. Ziolkowski, P. Schmidt, T. Marchenko, O. Travnikova, L. Journel, I. Ismail, E. Kukk, J. Niskanen, F. Trinter, C. Vozzi, M. Devetta, S. Stagira, M. Gisselbrecht, A. L. Jäger, X. Li, Y. Malakar, M. Martins, R. Feifel, L. Ph. H. Schmidt, A. Czasch, G. Sansone, D. Rolles, A. Rudenko, R. Moshammer, R. Dörner, M. Meyer, T. Pfeifer, M. S. Schöffler, R. Santra, M. Simon, and M. N. Piancastelli. Inner-Shell-Ionization-Induced Femtosecond Structural Dynamics of Water Molecules Imaged at an X-Ray Free-Electron Laser. *Phys. Rev. X*, 11(4):041044, December 2021.

[2] A. Rudenko, L. Inhester, K. Hanasaki, X. Li, S. J. Robatjazi, B. Erk, R. Boll, K. Toyota, Y. Hao, O. Vendrell, C. Bomme, E. Savelyev, B. Rudek, L. Foucar, S. H. Southworth, C. S. Lehmann, B. Kraessig, T. Marchenko, M. Simon, K. Ueda, K. R. Ferguson, M. Bucher, T. Gorkhover, S. Carron, R. Alonso-Mori, J. E. Koglin, J. Correa, G. J. Williams, S. Boutet, L. Young, C. Bostedt, S.-K. Son, R. Santra, and D. Rolles. Femtosecond Response of Polyatomic Molecules to Ultra-intense Hard X-rays. *Nature*, 546(7656):129–132, May 2017.

[3] Robin Santra. Concepts in x-ray physics. *J. Phys. B: At. Mol. Opt. Phys.*, 42(2):023001, December 2008.

[4] Sang-Kil Son and Robin Santra. Monte Carlo calculation of ion, electron, and photon spectra of xenon atoms in x-ray free-electron laser pulses. *Phys. Rev. A*, 85(6):063415, June 2012.

[5] Sang-Kil Son, Linda Young, and Robin Santra. Impact of hollow-atom formation on coherent x-ray scattering at high intensity. *Phys. Rev. A*, 83(3):033402, March 2011.

[6] L. Young, E. P. Kanter, B. Kraessig, Y. Li, A. M. March, S. T. Pratt, R. Santra, S. H. Southworth, N. Rohringer, L. F. DiMauro, G. Doumy, C. A. Roedig, N. Berrah, L. Fang, M. Hoener,

P. H. Bucksbaum, J. P. Cryan, S. Ghimire, J. M. Glownia, D. A. Reis, J. D. Bozek, C. Bost-edt, and M. Messerschmidt. Femtosecond electronic response of atoms to ultra-intense X-rays. *Nature*, 466(7302):56–61, July 2010.